

Calculation of direct-semidirect radiative proton capture with Skyrme-Hartree-Fock-BCS model

Takehito Watanabe^{1,a}, Toshihiko Kawano¹, and Ludovic Bonneau²

¹ Theoretical Division, Los Alamos National Laboratory, Los Alamos, New Mexico 87545, USA

² CENBG, Le Haut Vigneau, 33175 Gradignan, France

Abstract. We calculate the direct-semidirect (DSD) radiative proton capture cross section on ^{112}Sn , ^{63}Cu , and ^{209}Bi in the microscopic Hartree-Fock-BCS approach using the Skyrme interaction. Compared to the compound process, the DSD process becomes dominant in the proton capture reaction above ten and several MeV incident proton energies. We compare several particle-vibration coupling forms, which is sensitive to the semidirect cross section.

1 Introduction

The origin of the abundances of the elements is well understood through astrophysical r - and s -processes. However, there exist significant uncertainties for the so-called p -nuclei, which cannot be produced via the neutron capture processes. When nucleosynthesis occurs in hydrogen-rich compositions, the nuclear burning proceeds via the rapid proton capture process (rp -process), and a sequence of proton captures and β^+ decays are responsible for the burning of hydrogen into heavier elements. The proton radiative capture, therefore, plays an important role in nucleosynthesis calculations in astrophysics.

The nucleon radiative capture can be described by the compound and the direct-semidirect (DSD) processes[1, 2]. In the compound reaction, which is calculated by the statistical Hauser-Feshbach model with width fluctuation correction[3], the proton capture cross section starts to decrease rapidly when the (p,n) reaction channel opens, because the neutron width Γ_n becomes much larger than the gamma-ray width Γ_γ . Above the (p,n) reaction threshold, therefore, the capture process can be mainly described by the DSD mechanism. In this mechanism, the incident particle is captured directly in an unoccupied bound state (direct), or it excites a collective (giant dipole resonance) state and then is scattered into a bound state (semidirect).

Within the perturbation theory, the transition probabilities of the DSD processes involve radial wave functions and spectroscopic factors of the final states. Because the experimental information on nuclear structure for unstable nuclei is often uncertain or unavailable, we have to rely on model calculations to determine the DSD cross section. Therefore, we developed a DSD model based on the Hartree-Fock-BCS (HFBCS) model[4–6] using the Skyrme force to calculate the radial wave-functions of the single-particle (sp) bound states of even-even target nuclei and

their associated occupation probabilities from which we deduce the spectroscopic factors as in Refs. [7, 8]. In this work, we apply our HFBCS model to calculating the DSD proton capture on odd- and even- Z nuclei (with even- N).

We have to apply the HFBCS model to even-even nuclei. Therefore, in the odd- Z target case we consider an even-even residual nucleus formed by the proton capture reaction on the odd target. The spectroscopic factors of the odd- Z target sp states can be related to the proton occupation probabilities for the residual nucleus.

2 Calculation

2.1 Direct-semidirect cross section

Let us consider an incident nucleon with wave number k_n and orbital and total angular momenta L and J , respectively. This nucleon is directly captured into a bound state $|k\rangle$. Assuming that the target is deformed with axial symmetry, the sp wave function $|k\rangle$ is an eigenstate of J_z , the projection on the symmetry axis of the angular momentum operator \mathbf{J}^2 . The associated eigenvalue is denoted by K . The deformed sp state $|k\rangle$ is a superposition of eigenstates of the orbital and total angular momentum operators \mathbf{L}^2 and \mathbf{J}^2 , respectively:

$$|k\rangle = \sum_{lj} C_{lj}^{(k)} |ljK\rangle. \quad (1)$$

The corresponding partial DSD nucleon capture cross section is calculated as a sum of two coherent amplitudes[9, 10],

$$\sigma^{(k)}(lj; LJ) = \frac{16\pi}{9} \frac{\mu k_\gamma^3}{\hbar^2 k_n^3} |T_d^{(k)}(lj; LJ) + T_{sd}^{(k)}(lj; LJ)|^2, \quad (2)$$

where T_d and T_{sd} denote the direct and semidirect amplitudes, μ is the reduced mass of the projectile-target system,

^a e-mail: watanabe@lanl.gov

and k_n and k_γ are the wave numbers of the projectile and emitted γ -ray. The direct amplitude is written as

$$T_d^{(k)}(lj; LJ) = \bar{e}(-i)^{l+1} \frac{1}{\sqrt{2j+1}} Z(LJlj; \frac{1}{2}1) \times \sqrt{S_{lj}^{(k)}} \langle \mathcal{R}_{lj}^{(k)}(r) | r | R_{LJ}(r) \rangle, \quad (3)$$

where \bar{e} is the effective charge ($\bar{e} = -Ze/A$); $R_{LJ}(r)$, the radial part of distorted wave function with orbital and total angular momenta L and J ; $\mathcal{R}_{lj}^{(k)}(r)$, the radial part of sp wave function $|k\rangle$; $S_{lj}^{(k)}$, the spectroscopic factor; and $Z(LJlj; \frac{1}{2}1)$, the Z coefficient[11] that gives the selection rule of angular momenta. $R_{LJ}(r)$ is calculated with the optical model (OM). We adopt a global OM potential by Koning and Delaroche[12], which gives the potential for a wide range of nuclides. As for the semidirect amplitude, it is given by

$$T_{sd}^{(k)}(lj; LJ) = \pm \frac{3}{2\langle r^2 \rangle} \frac{N^2 Z^2}{A^3} e \sum_{l'j'} \left[(-i)^{l'+1} \frac{1}{\sqrt{2j'+1}} \times Z(LJl'j'; \frac{1}{2}1) \sqrt{S_{l'j'}^{(k)}} \langle \mathcal{R}_{l'j'}^{(k)}(r) | h(r) | R_{LJ}(r) \rangle \times \sum_{\nu} \langle 1-\nu, J, \nu+K | j'K \rangle \langle 1-\nu, J, \nu+K | jK \rangle \times \frac{|\langle \psi_{1\nu} | \rho'_\nu | \psi_{00} \rangle|^2}{E_n - (E_\nu + \epsilon) + i\frac{1}{2}\Gamma_\nu} \right], \quad (4)$$

where $\langle r^2 \rangle$ is the mean square radius; $h(r)$, the nucleon-nucleus vibration coupling function; ϵ , the sp energy of the bound state; E_ν and Γ_ν , the giant dipole resonance (GDR) energy and width, respectively; and the index ν , the GDR modes corresponding to major and minor axes. When $h(r)$ is a surface form[9], the factor $3/\langle r^2 \rangle$ must be omitted[13]. The transition matrix element between the dipole and ground states $|\langle \psi_{1\nu} | \rho'_\nu | \psi_{00} \rangle|^2$ can be related to a photoabsorption cross section[9, 10]. The GDR parameters are taken from experimental data, or are calculated with a simple systematics[14] obtained from the experimental database. Finally, summing up all contributions from the bound states and their (l, j) components, the total DSD cross section is obtained.

As for the particle-nucleus vibration coupling function $h(r)$ in Eq. (4), to which the semidirect capture cross section is sensitive, we consider three types of the function form: the complex function with the values $V_1 = 75$ and $W_1 = 140$ MeV proposed by Potokar[15], the real function forms $V_1 df(r)/dr$ ($V_1 = 170$ MeV) by Boisson and Jang[9] and $V_1 rf(r)$ ($V_1 = 110$ MeV) by Kitazawa et al.[10], where $f(r)$ is the Woods-Saxon form.

2.2 Radial wave function and spectroscopic factors within Hartree-Fock-BCS approach

Single-particle states in a nucleus are calculated with the HFBCS model using two different parametrizations of the

Skyrme effective force, together with traditionally associated pairing interactions used in the BCS approximation. One is the SLy4 parameterization [16] with the density-dependent delta interaction (DDDI) [17, 18] as a pairing interaction. Secondly, the seniority force (constant matrix elements between pairs of time reversed states) is chosen as a pairing interaction while using the Skyrme SIII parameterization[19] as a Skyrme force. The strengths of the seniority force for neutrons and protons are the same as those used in Ref. [20].

Using these pairs of forces, we solve the Skyrme-HF equation[21, 22] to obtain the deformed sp wave function. Owing to the axial symmetry assumed here, we perform the HF Hamiltonian diagonalization in the cylindrical harmonic-oscillator (HO) basis and then expand it onto the spherical HO basis (see Ref. [6] for detail). The radial part of deformed sp state $|k\rangle$ can be expressed as

$$\mathcal{R}_{lj}^{(k)}(r) = \sum_{n \geq} s_{nlj}^{(k)} R_{nl}(r), \quad (5)$$

where R_{nl} is the radial part of spherical HO wave function. $C_{lj}^{(k)}$ in Eq. (1) is related with $s_{nlj}^{(k)}$ as

$$|C_{lj}^{(k)}|^2 = \sum_{n \geq} |s_{nlj}^{(k)}|^2. \quad (6)$$

Finally, the spectroscopic factor $S_{ij}^{(k)}$ is given by

$$S_{ij}^{(k)} = \begin{cases} \frac{2u_k^2}{2j+1} |C_{lj}^{(k)}|^2 & \text{for odd-even target} \\ 2v_k^2 |C_{lj}^{(k)}|^2 & \text{for even-even target,} \end{cases} \quad (7)$$

where u_k^2 and v_k^2 are the vacancy and occupation probabilities in the BCS model.

3 Results

We performed the DSD model calculation with the HFBCS bound states for ^{112}Sn (even-even), ^{63}Cu and ^{209}Bi (odd-even). In the $^{63}\text{Cu}(p, \gamma)^{64}\text{Zn}$ and $^{209}\text{Bi}(p, \gamma)^{210}\text{Po}$ reactions, the Skyrme-HFBCS model was applied to the residual nuclei.

Figure 1 shows the DSD proton capture cross sections on ^{112}Sn calculated using the SIII (dashed line) and SLy4 (solid line) Skyrme forces, respectively. Here, the complex form factor of Potokar was used as the coupling form factor. In this figure, the compound nucleus (CN) cross section calculated by CoH[23] is shown (dotted line) to make a comparison between the compound and DSD components of proton radiative capture. The dot-dashed curve represents a sum of the CN and DSD cross sections. The (p,n) reaction cross section is also shown (two-dot-dashed line). The calculation of CN cross section is in close agreement with the experimental data[24] below the (p,n) reaction threshold. Above the (p,n) threshold energy, the CN cross section decreases rapidly with the incident proton energy, and above 17 MeV the DSD cross section becomes

dominant in the proton capture reaction. The two DSD calculations with SIII and SLy4 give almost the same results.

Figures 2 and 3 show the DSD calculation results for $^{63}\text{Cu}(p,\gamma)$ and $^{209}\text{Bi}(p,\gamma)$, respectively. The Potokar type of coupling form factor was employed here. In Fig. 2, the CN cross section calculation is in good agreement with the experimental data of Sevier et al.[25] and keeps to be dominant up to 20 MeV. The experimental data of Drake et al.[26] support our DSD calculation because the reproduction of experimental data is improved by the CN plus DSD cross sections in a range of 6 to 11 MeV, but at higher energies there are some discrepancies. In Fig. 3, the DSD component dominates the proton capture reaction above 12 MeV. The calculation of CN + DSD cross section has a shape consistent with the experimental values of Daly and Shaw, but the absolute values are smaller by almost an order of magnitude.

We also performed the DSD calculation choosing the various types of coupling form function $h(r)$ mentioned above. Figures 4 and 5 show the calculated results of total cross section (CN + DSD) of $^{63}\text{Cu}(p,\gamma)$ and $^{209}\text{Bi}(p,\gamma)$ reactions: Potokar (dot-dashed line), Kitazawa (solid line), and Boisson and Jang form factors (dashed line). The CN cross sections are also shown in these figures by the dotted line. In Fig. 4, the form factor of Boisson and Jang gives better agreement with measurement values of Drake et al. above 14 MeV. In Fig. 5, above 9 MeV the Boisson and Jang's form factor improves the reproduction of experimental data of Daly and Shaw. The form factors of Kitazawa and Potokar give very similar cross sections for both cases.

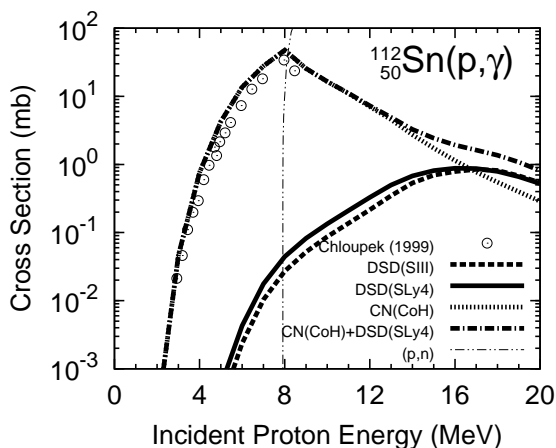


Fig. 1. Calculated results of DSD proton capture cross section on ^{112}Sn . The dashed and solid lines represent the DSD calculations using the SIII and SLy4 Skyrme forces, respectively. A compound nucleus (CN) cross section calculated by CoH is shown by the dotted line. The one-dot-dashed line is the CN plus DSD (SLy4) cross section. The (p,n) reaction cross section by CoH is also shown by the two-dot-dashed line. The experimental data were taken from Ref. [24].

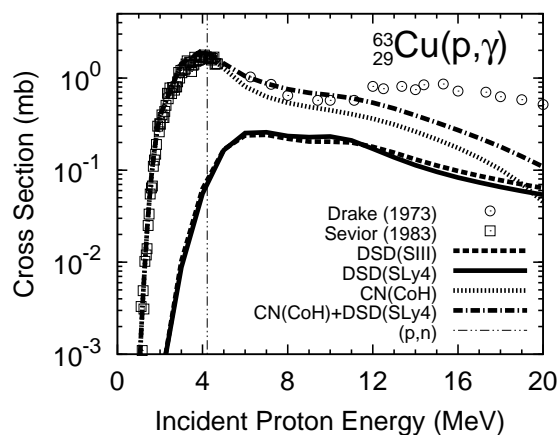


Fig. 2. The same as Fig. 1 for $^{63}\text{Cu}(p,\gamma)$. The experimental data were taken from Refs. [26, 25].

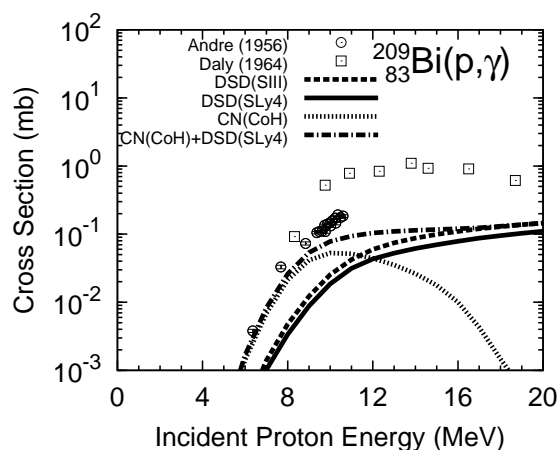


Fig. 3. The same as Fig. 1 for $^{209}\text{Bi}(p,\gamma)$. The experimental data were taken from Refs.[27, 28].

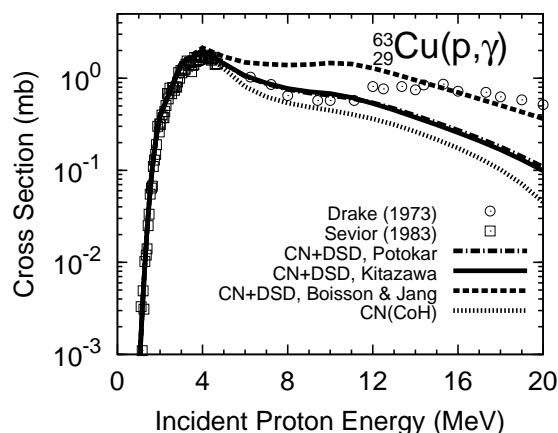


Fig. 4. Comparison of total (CN + DSD) cross section calculation for $^{63}\text{Cu}(p,\gamma)$ using various types of coupling form factor $h(r)$.

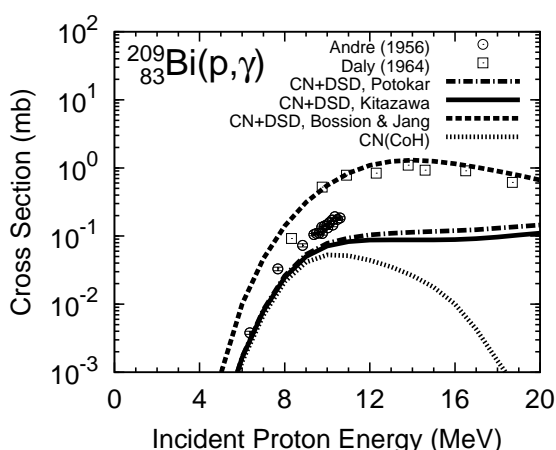


Fig. 5. The same as Fig. 4 for $^{209}\text{Bi}(p,\gamma)$.

4 Conclusions

We proposed a new method for calculating the DSD proton radiative capture cross section. The *sp* bound states and their spectroscopic factors are calculated within the Skyrme-HFBCS model. This method was applied to ^{112}Sn , ^{63}Cu , and ^{209}Bi . We found that the DSD process dominates in the proton capture above 17 and 12 MeV for ^{112}Sn and ^{209}Bi , respectively. In $^{63}\text{Cu}(p,\gamma)$, whereas the CN process mainly contributes to the total capture cross section, the experimental data implies importance of the DSD process. If the particle-vibration coupling proposed by Bossion and Jang is used, the CN + DSD cross section calculation fairly reproduces the experimental data of $^{63}\text{Cu}(p,\gamma)$ and $^{209}\text{Bi}(p,\gamma)$.

Acknowledgments

This work was carried out under the auspices of the National Nuclear Security Administration of the U.S. Department of Energy at Los Alamos National Laboratory under contract No. DE-AC52-06NA25396.

References

- G. E. Brown, Nucl. Phys. **57**, (1964) 339.
- C. F. Clement, A. M. Lane, and J. R. Rook, Nucl. Phys. **66**, (1965) 273.
- R. Rauscher, F.-K. Thielemann, and K.-L. Kratz, Nucl. Phys. **A621**, (1997) 331c.
- T. Watanabe, L. Bonneau, and T. Kawano, Proc. of the 11th Int. Conf. on Nuclear Reaction Mechanisms, 12–16 June, 2006, Villa Monastero, Varenna, Italy, edited by E. Gadioli, Ricerca Scientifica ed Educazione Permanente Supplemento **No.126**, (2006) 85.
- L. Bonneau, T. Kawano, T. Watanabe, and S. Chiba, Proc. of the Int. Conf. on Nuclear Data for Science and Technology, 22–27 April, 2007, Nice, France, editors O. Bersillon, F. Gunsing, E. Bauge, R. Jacqmin, and S. Leray, EDP Sciences, 2008, pp 186–190.
- L. Bonneau, T. Kawano, T. Watanabe, and S. Chiba, Phys. Rev. **C75**, (2007) 054618.
- S. Yoshida, Phys. Rev. **123**, (1961) 2122.
- B. L. Cohen and R. E. Price, Phys. Rev. **121**, (1961) 1441.
- J. P. Boisson and S. Jang, Nucl. Phys. **A189**, (1972) 334.
- H. Kitazawa, T. Hayase, and N. Yamamuro, Nucl. Phys. **A307**, (1978) 1.
- L. C. Biendenharn, J. M. Blatt, and M. E. Rose, Rev. Mod. Phys. **24**, (1952) 249.
- A. J. Koning and J. P. Delaroche, Nucl. Phys. **A713**, (2003) 231.
- G. Longo and F. Saporetti, Nucl. Phys. **A199**, (1973) 530.
- T. Belgya, O. Bersillon, R. Capote, T. Fukahori, G. Zhigang, S. Goriely, M. Herman, A. V. Ignatyuk, S. Kailas, A. J. Koning, P. Obložinský, V. Plujko, and P. G. Young, “Handbook for calculations of nuclear reaction data, RIPL-2,” IAEA-TECDOC-1506, International Atomic Energy Agency (2006); available online at <http://www-nds.iaea.org/RIPL-2/>.
- M. Potokar, Phys. Lett. **B46**, (1973) 346.
- E. Chabanat, P. Bonche, P. Haensel, J. Meyer, and R. Schaeffer, Nucl. Phys. **A635**, (1998) 231.
- C. Rigollet, P. Bonche, H. Flocard, and P.-H. Heenen, Phys. Rev. **C59**, (1999) 3120.
- T. Duguet, P. Bonche, and P.-H. Heenen, Nucl. Phys. **A679**, (2001) 427.
- M. Beiner, H. Flocard, N. Van Giai, and P. Quentin, Nucl. Phys. **A238**, (1975) 29.
- L. Bonneau, Phys. Rev. **C74**, (2006) 014301.
- D. Vautherin and D. M. Brink, Phys. Rev. **C5**, (1972) 626.
- D. Vautherin, Phys. Rev. **C7**, (1973) 296.
- T. Kawano, “The Hauser–Feshbach–Moldauer statistical model with the coupled channels theory,” [unpublished].
- F. R. Chloupek, A. StJ. Murphy, R. N. Boyd, A. L. Cole, J. Görres, R. T. Guray, G. Raimann, J. J. Zack, T. Rauscher, J. V. Schwarzenberg, P. Tischhauser, and M. C. Wiescher, Nucl. Phys. **A652**, (1999) 391.
- M. E. Sevier, L. W. Mitchell, M. R. Anderson, C. W. Tingwell, D. G. Sargood, Aust. J. Phys. **36**, (1983) 463.
- D. M. Drake, S. L. Whetstone, and I. Halpern, Nucl. Phys. **A203**, (1973) 257.
- C. G. Andre, J. R. Huizenga, J. F. Mech, W. J. Ramler, E. G. Rauh, and S. R. Rocklin, Phys. Rev. **101**, (1956) 645.
- P. J. Daly and P. F. D. Shaw, Nucl. Phys. **56**, (1964) 322.